International Journal of Biological Macromolecules 181 (2021) 858–867

Contents lists available at ScienceDirect

International Journal of Biological Macromolecules

journal homepage: http://www.elsevier.com/locate/ijbiomac

Structural and functional analysis of the simultaneous binding of two duplex/quadruplex aptamers to human α-thrombin

Romualdo Troisi [a], Nicole Balasco [b], Andreas Santamaria [a,1], Luigi Vitagliano [b], Filomena Sica [a,*]

[a] Department of Chemical Sciences, University of Naples Federico II, Complesso Universitario di Monte Sant'Angelo, Via Cintia, I-80126 Naples, Italy
[b] Institute of Biostructures and Bioimaging, CNR, Naples I-80134, Italy

ARTICLE INFO

Article history:
Received 19 March 2021
Received in revised form 12 April 2021
Accepted 13 April 2021
Available online 14 April 2021

Keywords:
Thrombin modulation
Anti-thrombin aptamer
Inter-exosite communication

ABSTRACT

The long-range communication between the two exosites of human α-thrombin (thrombin) tightly modulates the protein-effector interactions. Duplex/quadruplex aptamers represent an emerging class of very effective binders of thrombin. Among them, NU172 and HD22 aptamers are at the forefront of exosite I and II recognition, respectively. The present study investigates the simultaneous binding of these two aptamers by combining a structural and dynamics approach. The crystal structure of the ternary complex formed by the thrombin with NU172 and HD22_27mer provides a detailed view of the simultaneous binding of these aptamers to the protein, inspiring the design of novel bivalent thrombin inhibitors. The crystal structure represents the starting model for molecular dynamics studies, which point out the cooperation between the binding at the two exosites. In particular, the binding of an aptamer to its exosite reduces the intrinsic flexibility of the other exosite, that preferentially assumes conformations similar to those observed in the bound state, suggesting a predisposition to interact with the other aptamer. This behaviour is reflected in a significant increase of the anticoagulant activity of NU172 when the inactive HD22_27mer is bound to exosite II, providing a clear evidence of the synergic action of the two aptamers.

1. Introduction

Despite significant advances in the prevention and treatment of thrombosis expanding day-to-day, this disease is still one of the leading causes of death worldwide [1]. The anticoagulant drugs often used to control blood coagulation (heparin, warfarin, and bivalirudin) in many cases show adverse effects [2,3]. Oligonucleotide aptamers, DNA or RNA sequences able to bind with high affinity and selectivity a target molecule, have shown to be alternative specific anticoagulants, which are characterized by nonimmunogenicity and nontoxicity [4,5]. Interestingly, a subclass of these aptamers that adopts a G-quadruplex structure is able to effectively modulate the activity of the human α-thrombin (thrombin), a multifunctional trypsin-like serine protease that plays a pivotal role in the coagulation pathway [6,7].

In the last decades, various anti-thrombin aptamers were selected [8–17] against the two positively charged regions (known as exosite I and exosite II), which lie at opposite sides of the thrombin active site and regulate enzyme activity by binding substrates and cofactors [18–20]. TBA (also known as HD1) (5′-GGTTGGTGTGGTTGG-3′) is the most studied anti-thrombin aptamer. It adopts an antiparallel G-quadruplex structure and binds to the fibrinogen-binding site (exosite I) of the thrombin with high affinity [7,21]. NU172 (5′-CGCCTAGGTTG GGTAGGGTGGTGGCG-3′), the only anti-thrombin aptamer currently in Phase II of clinical trials, adopts a compact duplex/quadruplex architecture and shows a significantly higher potency as an anticoagulant with respect to TBA [7,22]. Like TBA [23], NU172 also embraces the exosite I with the two G-quadruplex lateral loops that interact with the protein residues by means of hydrogen bonds and/or hydrophobic interfaces. The presence in the thrombin-NU172 complex (thrombin^{NU172}) of additional interactions with respect to thrombin-TBA (thrombin^{TBA}) determines the improvement in the anticoagulant activity of the duplex/quadruplex aptamer [22]. Despite their excellent anticoagulant properties and the advent of new powerful aptamers [16,17,24,25], researchers are investigating several strategies to overcome some long-standing limitations of both TBA and NU172, as the short circulating half-life *in vivo* [26–35]. Interestingly, another duplex/quadruplex oligonucleotide, HD22, recognizes thrombin exosite II with very high affinity but without exerting a potent antithrombotic activity [9,24,36].

To elucidate the structure-activity relationships of these attractive compounds, extensive crystallographic studies have been performed on thrombin-aptamer complexes [22,23,33,36–43]. In particular, the recognition between the TBA aptamer and thrombin has been

* Corresponding author.
E-mail address: filomena.sica@unina.it (F. Sica).
[1] Present address: Institut Laue-Langevin, 71 Avenue des Martyrs, 38,042 Grenoble, Cedex 9, France; Departamento de Química Física, Facultad de Ciencias Químicas, Universidad Complutense de Madrid, Ciudad Universitaria s/n 28,040, Madrid, Spain.

https://doi.org/10.1016/j.ijbiomac.2021.04.076
0141-8130/

investigated both in binary [23,39] and ternary [42] complexes. On the other hand, the interactions of the therapeutically promising NU172 aptamer with thrombin have been investigated only in the framework of one-to-one binary complexes [22].

Since the function of thrombin is regulated by long-range effects induced by the interaction with cofactors, substrates, or inhibitors, allosteric interactions may be important for the thrombin activity modulation [44–56]. In this scenario, we here investigated, using a repertoire of different experimental and computational techniques, the impact that the binding of a truncated form of HD22 (HD22_27mer, 5′-GTCCGTGGTAG GGCAGGTTGGGGTGAC-3′) at the exosite II has on the binding and on the anticoagulant activity of NU172. In particular, we report the crystal structure of the ternary complex formed by the thrombin with both NU172 and HD22_27mer (thrombin$^{NU172\text{-}HD22_27mer}$), extensive molecular dynamics simulations of different thrombin/aptamer complexes, and anticoagulant activity experiments. Collectively, the findings reported in the present manuscript provide a clear and detailed picture of the cooperative action that NU172 and HD22_27mer exert on thrombin inhibition.

2. Material and methods

2.1. Materials and sample preparation

The human D-Phe-Pro-Arg-chloromethylketone (PPACK)-inhibited thrombin (for crystallization) and the active human a-thrombin (for anticoagulant activity experiments) were purchased from Haematologic Technologies (USA), while fibrinogen from human plasma and oligonucleotides were purchased from Sigma-Aldrich (United Kingdom). NU172 and HD22_27mer samples were dissolved in 10 mM sodium phosphate buffer pH 7.0 and 100 mM NaCl (for crystallization) or Phosphate Buffered Saline (PBS) (for anticoagulant activity experiments). To induce folding, all aptamer samples were annealed by heating to 90 °C for 5 min and then slowly cooling down in 50–60 min and storing at 20 °C overnight.

2.2. Crystallography

A standard protocol [42] has been followed for the preparation of the thrombin$^{NU172\text{-}HD22_27mer}$ complex in 10 mM sodium phosphate buffer pH 7.0 and 100 mM NaCl. Briefly, the ternary complex was prepared depositing a 2-fold molar excess of HD22_27mer onto a frozen sample of thrombin. The system was left for about 7 h at 4 °C. Then the solution was frozen again and a 2-fold molar excess of a NU172 solution was deposited onto it. The system was kept at 4 °C overnight. The final solution was extensively washed to remove the excess of the aptamers and was finally concentrated to about 8 mg mL^{-1}.

An initial screening of crystallization experiments was performed by hanging drop vapour diffusion method mixing 0.5 μL complex solution with 0.5 μL reservoir solution at 20 °C, reproducing the conditions reported in the literature for the crystallization of other aptamer-thrombin complexes [22,23,33,36–43]. After a fine optimization of the crystallization conditions, crystals suitable for X-ray diffraction data collection grew in 26% w/v PEG 3350, 0.2 M ammonium acetate and 0.1 M Bis-Tris pH 6.5 (Fig. S1).

Diffraction data were collected at the Institute of Biostructures and Bioimages (IBB), CNR, Naples, Italy, using a Rigaku Micromax 007 HF generator (CuKα radiation, λ = 1.5418 Å), equipped with a Saturn944 CCD detector. Crystal was cryoprotected by addition of 25% v/v ethylene glycol to the crystallization solution, flash-cooled at 100 K in supercooled N_2 gas and maintained at this temperature during the data collection. Crystals of the thrombin$^{NU172\text{-}HD22_27mer}$ complex belong to space group $P2_1$ and diffract X-ray up to 3.10 Å resolution. Matthews coefficient calculation suggested the presence of two ternary complexes in the asymmetric unit and a solvent content of 60.6%.

Dataset was processed using HKL2000 software [57]. The phase problem was solved by molecular replacement using Phaser MR [58] from the CCP4 package [59] and the coordinates of the native protein (PDB code: 1PPB) [60] as search model. The starting model was subjected to few cycles of rigid body refinement followed by several cycles of coordinate minimization and B-factor refinement using REFMAC5 program [61]. Analysis of Fourier difference maps and manual model building were performed with WinCoot program [62]. The final R_{factor}/R_{free} values were 0.200/0.257. Detailed statistics on data collection and refinement are reported in Table 1. The final model presents a good stereochemistry, as also indicated by the analysis of some conformation-dependent parameters such as the $NC^{\alpha}C$ (τ) angle and the deviation from the planarity of the ω dihedral angle (Table S1 and Fig. S2) [63–65].

The Superpose program [59,66] was used to calculate root-mean-square deviations (RMSD). Features of the thrombin-aptamer interfaces and interactions between the molecules were determined by PISA [59,67], DIMPLOT (LigPlot^{+} package) [68], and HBOND (http://cib.cf.ocha.ac.jp/bitool/HBOND/) programs. Molecular graphics figures were prepared with PyMOL (DeLano Scientific, Palo Alto, CA, USA). The coordinates of the thrombin$^{NU172\text{-}HD22_27mer}$ complex structure were deposited in the Protein Data Bank (code: 7NTU).

2.3. Molecular dynamics: models and protocols

All-atom MD simulations in explicit solvent were performed on the thrombin^{NU172} binary and thrombin$^{NU172\text{-}HD22_27mer}$ ternary complexes in the absence of PPACK at the active site. In detail the X-ray structure of NU172-bound thrombin (PDB code: 6GN7) [22] and the thrombin$^{NU172\text{-}HD22_27mer}$ complex 1 formed by protein chains AB, NU172 chain E and HD22_27mer chain G of the here reported crystal structure were used as starting models. Disordered regions (termini of the light chain, the C-terminal end of the heavy chain and the γ-autolysis loop) in these models were rebuilt using the unbound-thrombin structure (PDB code: 1PPB) as template. The endogenous sodium ion bound by the protein and that in the G-quadruplex motif of both aptamers were maintained in the starting models. The simulations of the free thrombin and the HD22_27mer-bound thrombin (thrombin^{HD22_27mer}) previously performed [56] were considered for comparative purposes.

Table 1
Crystallographic statistics for the thrombin$^{NU172\text{-}HD22_27mer}$ complex. Values in brackets refer to the highest resolution shell.

	Thrombin$^{NU172\text{-}HD22_27mer}$
Crystal data	
Space group	$P2_1$
Unit-cell parameters	
a, b, c (Å)	84.93, 77.62, 95.41
α, β, γ (deg)	90.00, 103.47, 90.00
V_M (Å^3 Da^{-1})	2.87
No. of complexes in the asymmetric unit	2
Solvent content (%)	60.6
Data collection	
Resolution limits (Å)	60.00–3.10 (3.21–3.10)
Unique reflections	22,065 (2150)
Completeness (%)	99.8 (99.8)
Average multiplicity	3.7 (3.7)
⟨I/σ(I)⟩	6.6 (2.2)
$CC_{1/2}$	1.0 (0.8)
Refinement	
Resolution limits (Å)	26.77–3.10
No. of reflections	20,946
R_{factor}/R_{free}	0.200/0.257
No. of atoms	6893
Average B factors (Å^2)	36.82
R.m.s. deviations	
Bond lengths (Å)	0.002
Bond angles (deg)	1.067
Ramachandran plot, residues in (%)	
Favoured regions	91.0
Allowed regions	9.0
Outliers	0
PDB code	7NTU

For the convenience of counting, thrombin residues were sequentially numbered from residue 1 to 36 for the light chain and from residue 37 to 295 for the heavy chain. For the correspondence between the MD (used in dynamics simulations) and CS (used in crystal structures) notations see [56].

It is worth recalling that thrombin exosites are not confined to a single protein segment but encompass non-consecutive regions of the polypeptide chain: residues 45 (CS 24), 104–111 (CS 73–79), 114 (CS 82), and 150 (CS 117) constitute exosite I whereas residues 121–134 (CS 89–101), 159–166 (CS 126–130), 205–210 (CS 164–169) and 280–293 (CS 232–245) belong to exosite II.

MD simulations were carried out with the GROMACS software [69] using Amber99sb as force field. The starting models were immersed in triclinic boxes solvated with water molecules of the TIP3P water model. Sodium counterions were added to balance negative charges (Table S2). Periodic boundary conditions were applied. All systems were initially energy minimized for 50,000 steps using steepest descent and then equilibrated at the temperature of 300 K for 500 ps and at the pressure of 1 atm for 500 ps. The Parrinello-Rahman [70] and the Velocity Rescaling [71] algorithms were applied to control pressure and temperature, respectively. A 10 Å cut-off was applied to account for Lennard-Jones interactions. The Particle Mesh Ewald (PME) [72] method was used to compute electrostatic interactions (grid spacing of 0.16 nm). Bond lengths were constrained with the LINCS method [73]. Simulations were run for 500 ns with a time step of 0.002 ps at constant temperature (300 K) and pressure (1 atm) (NpT ensemble).

The root-mean-square inner product (RMSIP) [74] values, computed on the protein C^{α} atoms between the two halves of the equilibrated trajectories (100–300 ns and 300–500 ns), indicate that the MD simulations reached an acceptable level of convergence (Table S2).

GROMACS routines [69] and the VMD program [75] were used to check the quality of trajectories and to perform structural analyses.

2.4. Anticoagulant activity experiments

The thrombin-induced clotting of fibrinogen was measured spectrophotometrically [76]. A 1.8 mg mL^{-1} solution of fibrinogen in PBS was placed in a PS cuvette to which the oligonucleotide(s) was (were) added up to a final concentration of 40 nM. After an equilibration of the solution in the instrument for 5 min, thrombin was added up to 5 nM. The time required for fibrin polymerization was determined from an UV scattering curve (380 nm) recorded over time. Each curve was determined in triplicate. The clotting time was derived from the maximum of the second derivative of each scattering curve. The basal clotting time was determined in the absence of oligonucleotides.

3. Results

The impact of the simultaneous binding of NU172 and HD22_27mer, a truncated variant of HD22 amenable for crystallographic studies, on thrombin structure, dynamics, and activity was here investigated by determining the crystallographic structure of the thrombin$^{NU172\text{-}HD22_27mer}$ ternary complex, by performing fully atomistic molecular dynamics (MD) simulations on binary (thrombin^{NU172}) and ternary (thrombin$^{NU172\text{-}HD22_27mer}$) complexes, and by measuring the anticoagulant activity of NU172 as function of the presence/absence of HD22_27mer.

3.1. Crystal structure of the thrombin$^{NU172\text{-}HD22_27mer}$ ternary complex

The thrombin$^{NU172\text{-}HD22_27mer}$ ternary complex was crystallized by adapting and fine-tuning the experimental conditions used for other thrombin-aptamer complexes. To avoid protein autodigestion and consequently guarantee the homogeneity of the sample, the crystallization experiments were performed using a thrombin sample in which the active site was blocked by the covalent inhibitor PPACK. Crystals of thrombin$^{NU172\text{-}HD22_27mer}$ suitable for crystallographic analyses belong to the monocline space group $P2_1$ and diffract X-rays up to 3.10 Å resolution. The asymmetric unit contains two ternary complexes (denoted as complex 1 and 2) in which, as expected, NU172 binds the thrombin exosite I while HD22_27mer binds exosite II located on the opposite side of thrombin molecule. The final refined model of both complexes lacks some residues at light chain termini, Gly246 and Glu247 at the heavy chain C-terminus, and Thr147-Lys149e at the γ-autolysis loop. NU172 and HD22_27mer aptamers could be entirely traced in both complexes. The two complexes in the asymmetric unit form an intricate pattern of contacts with symmetry-related mates mediated by the aptamers that generates a crystal-wide array of interacting complexes (Fig. 1). Complexes 1 and 2 present a similar architecture, as also shown by the value of the root-mean-square deviation (RMSD, 0.42 Å) calculated after the superposition of the C^{α} protein atoms and all oligonucleotide atoms. Hence, the complex 1 will be referred to throughout the text unless stated otherwise.

Thrombin structure has been carefully examined and compared with that adopted in the unbound state and in the thrombin^{NU172} and thrombin^{HD22_27mer} binary complexes. In particular, the RMSD values after the superposition of all the C^{α} thrombin atoms with those of the aptamer-free protein (PDB code: 1PPB) [60], NU172-bound protein (PDB code: 6GN7) [22], and HD22_27mer-bound protein (PDB code: 4I7Y) [36] resulted 0.48 Å, 0.51 Å, and 0.45 Å, respectively. This analysis clearly indicates that the protein overall structure is essentially invariant despite the different binding states. Moreover, residues of both exosites adopt conformations that are similar to those found in the other crystallographic models of both free and liganded thrombin. It cannot be excluded that this finding is due to the presence, in the thrombin active site of all these structures, of the PPACK inhibitor that has been reported to influence the intrinsic mobility of the protein [77,78].

As concerns aptamers, NU172 assumes a compact mixed duplex/quadruplex architecture, which is very similar to that previously found

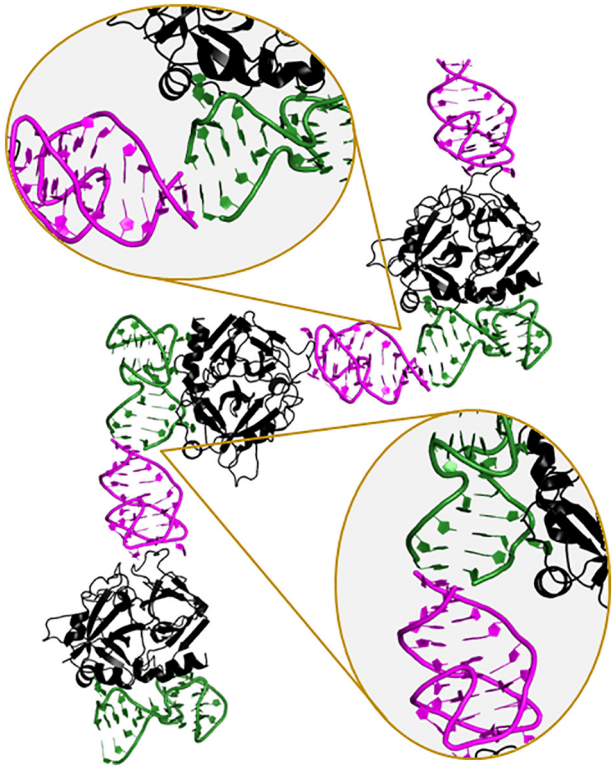

Fig. 1. Details of the interaction between aptamers in the crystal packing of thrombin$^{NU172\text{-}HD22_27mer}$ ternary complex. Thrombin, NU172, and HD22_27mer are black, magenta, and green, respectively.

in the thrombin^{NU172} binary complex (Fig. S3). Although retaining a duplex/quadruplex folding (Fig. S4), HD22_27mer presents some small conformational variations when compared to the structure it adopts in the thrombin^{HD22_27mer} binary complex. In particular, the tetrad II (Gua5, Gua7,Gua12,Gua16) of HD22_27mer G-quadruplex domain adopts a non-canonical organization, where all guanines are in the anti-conformation (Fig. 2). This organization differs from that found in the binary complex and is similar to that observed for the two previously reported [42] ternary complexes where exosite I was bound to TBA variants. This organization allows a more massive presence of a sodium ion between the two tetrads of HD22_27mer G-quadruplex domain (Fig. 2), which is present at a very low level in the thrombin^{HD22_27mer} binary complex. Moreover, the Gua13 and Cyt14 nucleobases that stack on HD22_27mer G-quadruplex tetrad II are flipped with respect to all other previously reported crystal structures, binary and ternary complexes, of HD22_27mer (Fig. 3). All these features underline significant differences on the intrinsic nature of the two aptamers. Indeed, NU172 is able to fold in a very packed structure thanks to a continuous stacking between the duplex and the quadruplex domains. On the contrary, HD22_27mer is a more flexible aptamer and its conformation is strongly influenced by the boundary conditions. This is also supported by the finding that some residues (Gua23-Thy24-Gua25) of HD22_27mer could assume alternative conformations in the complex 2 of the here reported crystal structure.

Overall, the interaction mechanism of the two aptamers with thrombin is conserved with respect to the two binary complexes. A comparison of the buried areas, the hydrogen bonds, and the hydrophobic interactions is reported in Table S3.

It is worth mentioning that in thrombin$^{TBA\text{-}HD22_27mer}$ ternary complexes the modifications observed in the tetrad II with respect to thrombin^{HD22_27mer} are transmitted up to the protein recognition site and produce an increase of the contact area [42]. The rearrangement of the tetrad II in thrombin$^{NU172\text{-}HD22_27mer}$ does not generate similar variations at the protein-aptamer interface. It is likely that these effects are produced by crystal packing contacts as those detected in thrombin$^{NU172\text{-}HD22_27mer}$ (Fig. 1).

3.2. Molecular dynamics simulations on the thrombin$^{NU172\text{-}HD22_27mer}$ and thrombin^{NU172} complexes

In order to achieve a dynamic view of the recognition process between the thrombin and these two aptamers, MD simulations were performed on the thrombin$^{NU172\text{-}HD22_27mer}$ ternary complex. Moreover, to unravel mutual long-distance influences between the two exosites, the structural/dynamic behaviour of the two exosites in the ternary complex was compared to that observed in the related binary complexes. Since we have already reported MD simulations of the thrombin^{HD22_27mer} binary complex [56], to complete the picture we here performed MD studies also on the thrombin^{NU172} complex.

3.2.1. Structural stability of the systems in the MD simulations

MD simulations were performed in explicit solvent using the GROMACS package [69]. The crystallographic structure of the ternary complex described in the previous section was used as the starting model of the thrombin$^{NU172\text{-}HD22_27mer}$ complex. For the simulation of the binary complex, the crystallographic structure of thrombin^{NU172} (PDB code: 6GN7) was used as the starting model.

To assess the structural stability of the complexes in the crystal-free environment, we preliminarily monitored the time evolution of several indicators commonly used in MD studies as the RMSD values of trajectory structures compared to the starting models, the gyration radius, and specific structural parameters including distances and angles. As shown in Fig. 4, the systems reach a stable state within 50 ns of the simulation timescale with average RMSD values in the range 2.5–3.5 Å. Additionally, they do not show significant variations (<1 Å) in their gyration radius (Fig. S5).

Despite some limited fluctuations (<2.5 Å), the distance between the centres of mass of the protein and the aptamer(s) is well-preserved in the binary/ternary complexes (Fig. S6A, B). In addition, no significant variations (<8°) in the angle between the centres of mass of the partners in the ternary complex (156° in the starting model) are observed (Fig. S6C).

Overall, these results indicate that thrombin^{NU172} and thrombin-$^{NU172\text{-}HD22\_27mer}$ complexes do not undergo major structural reorganizations when analysed in a crystal-free context through MD simulations.

Once assessed the overall stability of the complexes in the MD simulations, we analysed specific structural features of the individual partners, *i.e.* the protein and the aptamer(s), within the complex. The protein/aptamer gyration radius values of the trajectory frames are in line with those detected in the crystallographic structures of thrombin (~18 Å), NU172 (~12 Å), and HD22_27mer (~14 Å) (Fig. S7). Also, the number of intramolecular H-bonds (~230 for thrombin, ~35 for NU172, and ~33 for HD22_27mer) is well-preserved throughout the

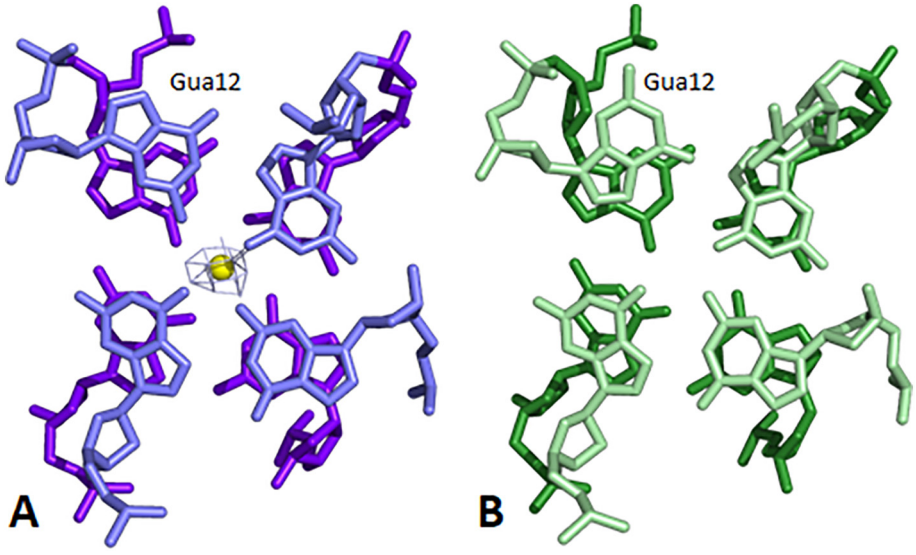

Fig. 2. View of the two tetrads along the G-quadruplex axis of HD22_27mer aptamer in A) thrombin$^{NU172\text{-}HD22_27mer}$ ternary complex and B) thrombin^{HD22_27mer} binary complex (PDB code: 4I7Y). Flipped guanine is labelled. The $2F_o$-F_c electron density map of the sodium ion (yellow) in ternary complex is contoured at 1.5 σ level.

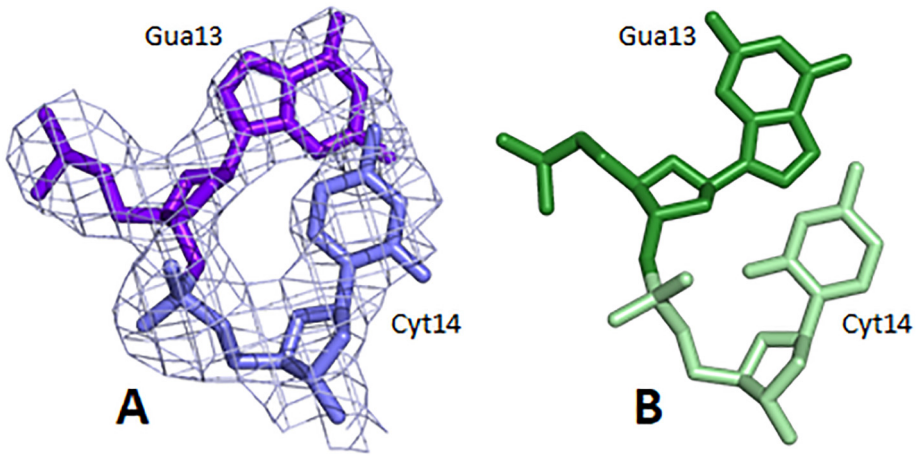

Fig. 3. View of Gua13 and Cyt14 of HD22_27mer aptamer in A) thrombin$^{NU172\text{-}HD22_27mer}$ ternary complex and B) thrombin^{HD22_27mer} binary complex (PDB code: 4I7Y). The $2F_o$-F_c electron density map in ternary complex is contoured at 1.0 σ level.

MD simulations. Finally, the good preservation of thrombin secondary structure elements in the simulation timescale confirms the protein structural stability (Fig. S8).

3.2.2. Dynamics of the protein-aptamer interactions in the MD simulations

The protein-aptamer interactions, both hydrophilic and hydrophobic (Table S3), that were found to stabilize the here determined crystallographic structure of the thrombin$^{NU172\text{-}HD22_27mer}$ ternary complex were analysed from a dynamic point of view.

As concerns thrombin-NU172 interface, the vast majority of the H-bonding interactions detected in the starting crystallographic models are either permanent or transient in the simulations of both the binary and ternary complexes (Table S4 and Fig. S9). It is also worth noting that some H-bonds, which are not present in the crystal structure of the binary complex but were found to stabilize the ternary complex, are formed throughout the MD simulation of thrombin^{NU172} (Table S4). *Vice versa*, interactions that are not detected in the crystal structure of the ternary complex but found in the crystal structure of thrombin^{NU172} are formed in the simulation of the thrombin$^{NU172\text{-}HD22_27mer}$ complex. This observation indicates that some of the differences emerged from the comparison of the crystal structures are due to the different packing environment and not to the different binding state of the thrombin. The preservation of the hydrophobic interactions that stabilize the thrombin-NU172 interface in the complexes has been also evaluated by computing the distances between the centres of mass of the residues/nucleotides involved in these contacts in the trajectory structures. Their time evolution indicates that a good level of preservation is achieved in the MD simulations (Table S4 and Fig. S9).

As concerns thrombin-HD22_27mer interface, a global analysis of the preservation of the intermolecular interactions in the ternary complex indicates that the H-bonds and hydrophobic contacts detected in the here reported crystallographic structure are well-conserved throughout the MD trajectory (Table S5 and Fig. S10). In addition, we observe the formation throughout the MD simulation of several H-bonds that were found to stabilize the system in the crystal structure of the binary complex.

3.2.3. Structural flexibility of the thrombin in the MD simulations

To gain insights into long-range communications in thrombin, we investigated the structural flexibility of the protein as derived from the MD simulations of thrombin^{NU172} and thrombin$^{NU172\text{-}HD22_27mer}$ complexes. These results were compared with those derived from the MD simulation we previously conducted [56] on the free protein.

We initially looked at the deviations of the average MD structure from the crystallographic starting model by computing the RMSD *per* residue values. As shown in Fig. S11, the highest displacements (RMSD values larger than 4 Å) are observed for the residues of the polypeptide chain termini and for the unstructured protein portions as the γ-autolysis loop, which encompasses MD residues 184–191 (CS residues 148–150). As expected, these regions also present large values of root-mean-square fluctuations (RMSF) (Fig. 5). As a consequence of the aptamer binding, lower RMSF values are shown by the ternary complex (violet) compared to the free protein (black). It is worth noting, however, that an increased rigidity is also observed for both exosites of thrombin^{NU172} binary complex (magenta). While the limited mobility of exosite I can be ascribed to NU172 anchoring, the rigidity of the

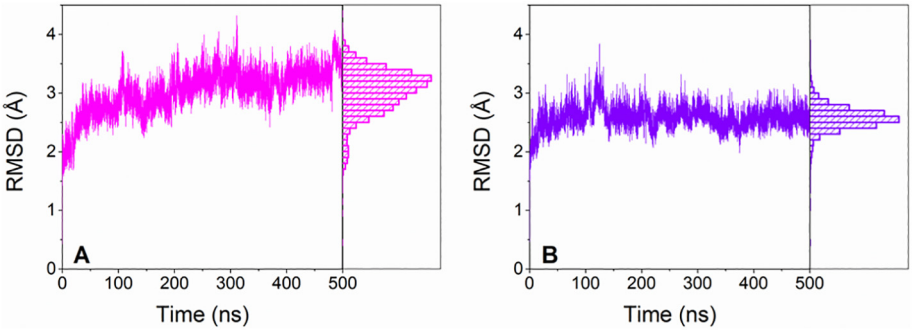

Fig. 4. RMSD values computed on all atoms of the trajectory structures against the starting crystallographic models for A) thrombin^{NU172} binary complex and B) thrombin$^{NU172\text{-}HD22_27mer}$ ternary complex. Distribution plots are reported on the right side of each plot.

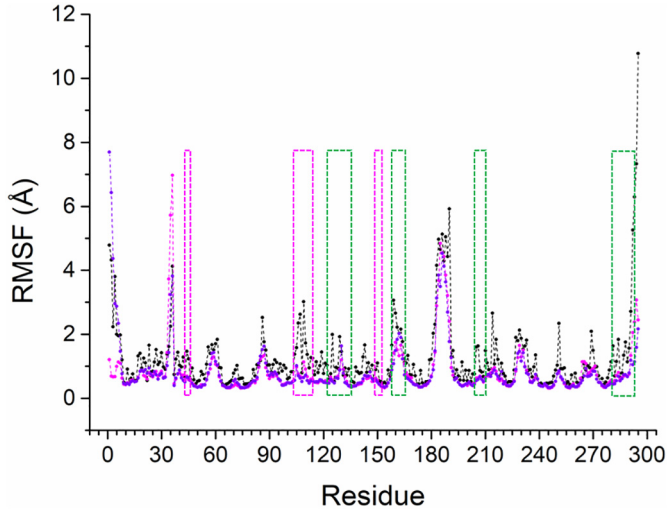

Fig. 5. RMSF values computed on thrombin C^{α} atoms in the 100–500 ns region of the MD trajectories in the simulations of free thrombin (black), of thrombin^{NU172} (magenta), and of thrombin$^{NU172\text{-}HD22_27mer}$ (violet). Magenta and green dashed boxes identify residues of exosites I and II, respectively.

unbound exosite II in this complex may suggest the possibility of long-range communications between exosites.

To gain further insights into this issue, we monitored the dynamical behaviour of the heavy chain C-terminal protein portion (MD residues 280–293, CS residues 232–245) that belongs to thrombin exosite II. As shown in Fig. 6A (left side), this region adopts the conformation of the free thrombin (black) in the starting crystallographic structure of the binary thrombin^{NU172} complex (magenta). On the other hand, a structural variation is observed in the X-ray model of the ternary thrombin$^{NU172\text{-}HD22_27mer}$ complex (violet) as shown by the position of the side chain of residue Phe293 (CS Phe245) which belongs to this protein region. To monitor the conformational behaviour of this portion we computed in the MD simulations the C^{α}-C^{α} distance between two residues, Phe280 (CS 232) and Phe293 (CS 245), that delimitate this exosite II segment (Fig. 6B). We previously [56] shown that this distance assumes a wide range of values (18–26 Å) in the trajectory frames of the unbound protein. Conversely, it is interesting to note that in thrombin^{NU172} trajectory structures preferentially adopt the values (in the range 19–21 Å) observed in the MD structures of the ternary complex with the exosite II bound by HD22_27mer (Fig. 6B). These data suggest that the binding of NU172 at the exosite I favors a conformational state of the exosite II that is prone to the anchoring of the other aptamer. The superimposition of the MD average structures on the right side of Fig. 6A clearly shows that in the simulation of the binary complex (magenta) the Phe293 evolves toward the state observed in the structure of the ternary complex (violet) where the exosite II is occupied. Altogether, these MD results support the idea of a remarkable cross-talk between the two thrombin exosites.

3.2.4. Structural flexibility of the aptamers in the MD simulations

The comparison of the crystal structures of NU172 and HD22_27mer has disclosed a different dynamic behaviour of the two aptamers. Indeed, while the structure of NU172 appears to be highly invariant as function of the context, on the other hand, Gua12 and Gua13 nucleobases of HD22_27mer are significantly reoriented in thrombin$^{NU172\text{-}HD22_27mer}$ when compared to their state in the thrombin^{HD22_27mer} binary complex (Figs. 2 and 3) and form different intramolecular interactions (Table S6). These nucleobases assume an intermediate state in the thrombin$^{TBA\text{-}HD22_27mer}$ ternary complex (Fig. S12). Using the MD simulation here performed on thrombin$^{NU172\text{-}HD22_27mer}$ and the simulations we previously conducted [56] on thrombin^{HD22_27mer} and thrombin$^{TBA\text{-}HD22_27mer}$ we evaluated the dynamic behaviour of these different states of HD22_27mer. The inspection of the total number of intramolecular H-bonds indicate that the HD22_27mer state detected in thrombin$^{NU172\text{-}HD22_27mer}$ is, on average, stabilized by a significantly higher number of bonds (Fig. S13). The inspection of the preservation of the interactions made by Gua12 clearly indicates that HD22_27mer

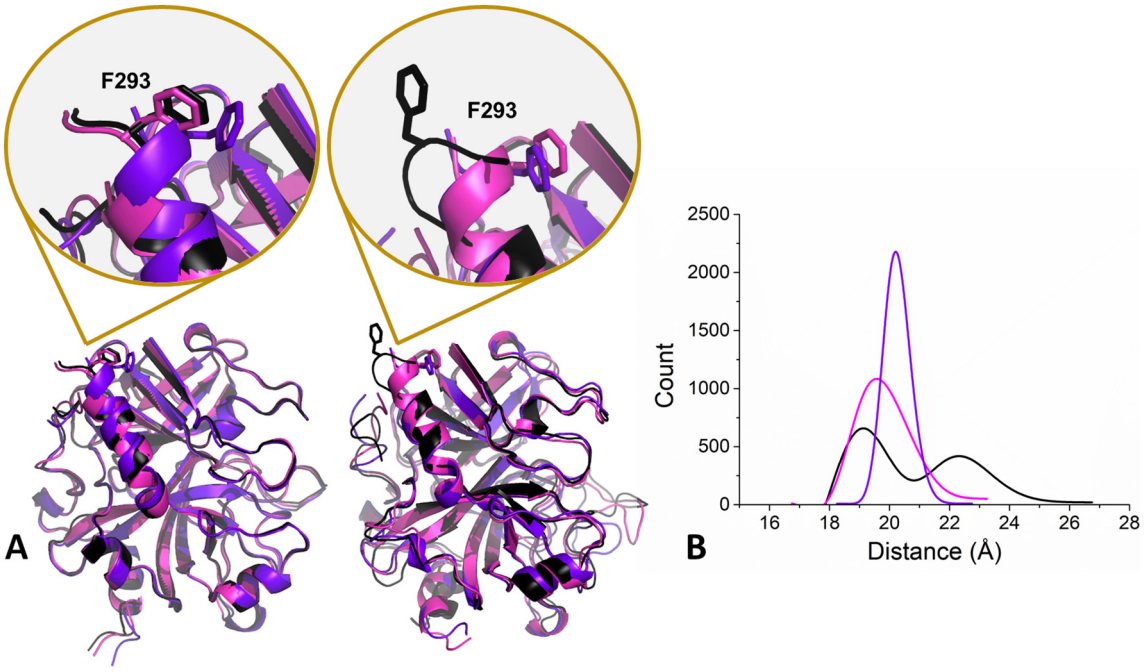

Fig. 6. A) Superimposition of the starting crystallographic structures (on the left) and the average structures computed in the region 100–500 ns of the MD simulations (on the right) of free thrombin (black), thrombin^{NU172} (magenta), and thrombin$^{NU172\text{-}HD22_27mer}$ (violet). The insets show the protein C-terminal region belonging to the exosite II. B) Distribution of the C^{α}-C^{α} distance of the exosite II residues Phe280 (CS 232) and Phe293 (CS 245) in the simulations of free thrombin (black), thrombin^{NU172} (magenta), and thrombin$^{NU172\text{-}HD22_27mer}$ (violet).

aptamer of thrombin$^{NU172\text{-}HD22_27mer}$ is significantly more rigid than that found in thrombin^{HD22_27mer} (Fig. S14). This guanine is also rigid in the aptamer of the thrombin$^{TBA\text{-}HD22_27mer}$ ternary complex. The analysis of the flexibility of Gua13 indicates that this nucleobase is mobile in the thrombin^{TBA_HD22_27mer} and thrombin^{HD22_27mer} complexes whereas it is rigid in the thrombin^{NU172_HD22_27mer} complex (Fig. S14). Collectively, these findings indicate that, compared to the structural states previously reported, the conformation of the HD22_27mer aptamer identified in the present study is stabilized by a larger number of H-bonds that confers to this state a remarkable rigidity.

3.3. Anticoagulant activity

Taking into account the indications emerged from the MD studies, we evaluated the ability of NU172 to compete with fibrinogen for thrombin exosite I in either the absence or presence on exosite II of HD22_27mer by performing a spectrophotometrical fibrinogen clotting assay. When HD22_27mer was bound to thrombin exosite II, a net enhancement of the anticoagulant activity of NU172 was revealed (Fig. 7). Instead, no variation of the anticoagulant activity of NU172 was detected in the presence of an equimolar amount of IGA3, an insulin binding aptamer that adopts a parallel G-quadruplex structure [79], used as negative control. It must be underlined that both HD22_27mer and IGA3 are not able to inhibit the cleavage of fibrinogen by thrombin, showing a clotting time comparable to the basal value determined in the absence of oligonucleotides (Fig. 7).

4. Discussion

The assessment of protein-ligand interactions is generally performed in terms of equilibrium binding affinities that significantly depend on the dynamics associated to the binding process. Indeed, the dynamic behaviour of the hot spot regions is frequently crucial for the recognition between biological partners. The structure of a binding site may be significantly affected by ligands and regulators that interact in distant regions of the protein (allostery). Frequently, the allosteric regulation does not produce discrete conformational rearrangements at the binding site, but it simply affects its dynamics [80]. This idea (dynamic allostery), developed by Cooper and Dryden [81] in 1984, has recently emerged as a new paradigm in the protein-ligand interaction field.

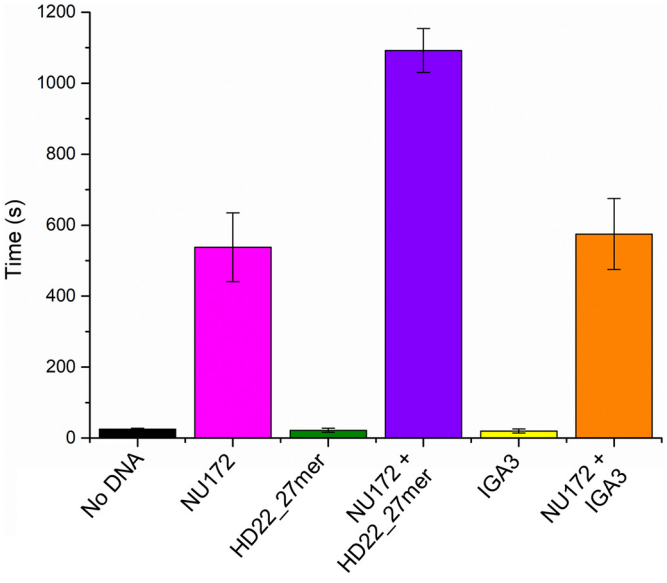

Fig. 7. Prolonged fibrinogen clotting times measured in PBS in the presence of fibrinogen (1.8 mg mL^{-1}), thrombin (5 nM), and aptamer(s) (40 nM). The basal clotting time in the absence of aptamers is also reported.

Allostery plays a crucial role in the activity and modulation of human α-thrombin as this protein can be fine regulated by the interaction with effectors binding at distant sites. Through-bond effects were also revealed between the two thrombin exosites and their typology is closely related to the nature of the interacting ligands [44–49,51,52,54]. It was found that, depending on the ligands, the binding at one exosite may either increase or reduce the affinity of interactors at the other. Interestingly, in the last decades, an aptamer-guided cooperation was observed between the two thrombin exosites [50,53,55]. Indeed, it was noted that the aptamer binding to exosite II increases the binding affinity of another aptamer to the fibrinogen-binding site (exosite I), and *vice versa*, consequently influencing the coagulant activity of the protein [24,82].

Recently, we found that the inter-exosite communication that follows the binding of TBA to exosite I or HD22_27mer to exosite II is mainly attributable to the reduction of the local dynamics that locked the two exosites in the aptamer-binding competent conformations [56]. In particular, the crystallographic analysis of the ternary complexes in which the protein is simultaneously bound to TBA variants and to HD22_27mer revealed that the presence of the aptamer at exosite I causes small but significant effects on the conformation and on the binding contacts of HD22_27mer [42].

In order to obtain further evidence of the aptamer-guided inter-exosite communication in thrombin, we have here studied the structure, the dynamics, and the functionality of the ternary complex in which thrombin is sandwiched between two duplex/quadruplex aptamers, NU172 and HD22_27mer.

From a structural point of view the comparison of the ternary complex under study with the corresponding binary ones indicates a reorganization of tetrad II in the case of HD22 _27mer, which is similar to that observed for the ternary complexes previously analysed [42]. Furthermore, the nucleobases Gua13 and Cyt14, which stack on tetrad II, adopt a novel conformation. The local structural variability of HD22_27mer, which has emerged from the crystallographic analyses hitherto conducted, highlights a higher conformational flexibility of this aptamer compared to both TBA and NU172. In particular, whereas NU172 has an elongated structure with very few contacts between its two structural domains, HD22_27mer assumes a peculiar sharply kinked conformation in which the helical axis of the duplex segment and that of the G-quadruplex motif are approximately perpendicular. This bent conformation gives more space to local structural fluctuations with respect to the elongated one.

To achieve a dynamic view of the thrombin interaction with aptamers, as done for other protein-aptamer complexes [83–85], and to obtain an unbiased view of the inter-exosite communication, we performed MD simulations on thrombin^{NU172} binary complex and thrombin$^{NU172\text{-}HD22_27mer}$ ternary complex and compared them with the simulations we previously conducted on the free protein and on thrombin^{HD22_27mer} and thrombin$^{TBA\text{-}HD22_27mer}$ complexes [56]. The analysis of the dynamics of the thrombin exosites in different contexts indicates that the binding of NU172 at the exosite I makes residues at the exosite II more rigid (Fig. 5). In particular, the binding of NU172 to exosite I favors conformations of the other site that are prone to the binding of HD22_27mer (Fig. 6). All these observations underline that the binding of an aptamer to a thrombin exosite mainly alters the dynamics of the other exosite, although it does not undergo to a net conformational change. In particular, the reduction of the mobility of the residues of the unbound exosite is associated with the selection of the conformation that is competent for the binding of the aptamer at that site.

To validate the findings emerged from the MD analyses, we evaluated the synergic action of the two aptamers in anticoagulation experiments (Fig. 7). Although HD22_27mer is not able to inhibit the cleavage of the fibrinogen to fibrin, its binding to the exosite II of the thrombin doubles the anticoagulant activity of NU172. Such an enhancement of NU172 activity is not observed in the presence of a 30mer oligonucleotide (IGA3) that does not bind the thrombin exosites. These

experimental results strongly corroborate the idea of a direct long-range correlation between the two exosites.

Overall, the present crystallographic and dynamic analyses have provided a detailed characterization of the modulation of the inter-exosite communication by anti-thrombin aptamers that has been corroborated by experimental data. The structural/dynamic data also highlight the different flexibility of the two aptamers. Indeed, while the structure of NU172 is strictly preserved in the complexes so far characterized, HD22_27mer somehow adapts its structure as function of the complex stoichiometry as well as of the crystal packing constraints.

In conclusion, the synergic action of the two aptamers here investigated represents an important stimulus for the design of bivalent thrombin-anchoring compounds [86–90]. Moreover, their tight association in the crystalline form of the ternary complex here characterized, mediated by the stacking of their duplex regions (Fig. 1) may provide clues for the rational design of monomolecular aptamers that are able to bind at once two different thrombin molecules, opening up to unexplored strategies of thrombin inhibition or detection.

Accession code

Coordinates and structure factors have been deposited in the Protein Data Bank under the accession code 7NTU.

Declaration of competing interest

The authors declare no conflict of interest.

Acknowledgements

Maurizio Amendola (IBB, CNR, Naples, Italy) is gratefully acknowledged for technical assistance during data collection. CINECA Supercomputing (framework ISCRA@CINECA - project code HP10C9HGRH) is acknowledged for computational support.

CRediT authorship contribution statement

Romualdo Troisi: Formal analysis, Investigation, Resources, Data curation, Writing - Original Draft, Writing - Review & Editing, Visualization. **Nicole Balasco**: Formal analysis, Data curation, Writing - Original Draft, Writing - Review & Editing. **Andreas Santamaria**: Investigation. **Luigi Vitagliano**: Conceptualization, Validation, Writing - Reviewing and Editing. **Filomena Sica**: Conceptualization, Validation, Resources, Writing - Review & Editing, Visualization, Supervision, Project administration.

Appendix A. Supplementary data

Supplementary data to this article can be found online at https://doi.org/10.1016/j.ijbiomac.2021.04.076.

References

[1] ISTH Steering Committee for World Thrombosis Day, Thrombosis: a major contributor to the global disease burden, J. Thromb. Haemost. 12 (2014) 1580–1590, https://doi.org/10.1111/jth.12698.
[2] M. Alquwaizani, L. Buckley, C. Adams, J. Fanikos, Anticoagulants: a review of the pharmacology, dosing, and complications, Curr. Emerg. Hosp. Med. Rep. 1 (2013) 83–97, https://doi.org/10.1007/s40138-013-0014-6.
[3] J.H. Kim, K.-M. Lim, H.S. Gwak, New anticoagulants for the prevention and treatment of venous thromboembolism, Biomol. Ther. 25 (2017) 461–470, https://doi.org/10.4062/biomolther.2016.271.
[4] H. Sun, Y. Zu, A highlight of recent advances in aptamer technology and its application, Molecules 20 (2015) 11959–11980, https://doi.org/10.3390/molecules200711959.
[5] J. Zhou, J. Rossi, Aptamers as targeted therapeutics: current potential and challenges, Nat. Rev. Drug Discov. 16 (2017) 181–202, https://doi.org/10.1038/nrd.2016.199.
[6] C. Roxo, W. Kotkowiak, A. Pasternak, G-Quadruplex-forming aptamers—characteristics, applications, and perspectives, Molecules 24 (2019)https://doi.org/10.3390/molecules24203781.
[7] C. Riccardi, E. Napolitano, C. Platella, D. Musumeci, D. Montesarchio, G-quadruplex-based aptamers targeting human thrombin: discovery, chemical modifications and antithrombotic effects, Pharmacol. Ther. 217 (2021), 107649, https://doi.org/10.1016/j.pharmthera.2020.107649.
[8] L.C. Bock, L.C. Griffin, J.A. Latham, E.H. Vermaas, J.J. Toole, Selection of single-stranded DNA molecules that bind and inhibit human thrombin, Nature 355 (1992) 564–566, https://doi.org/10.1038/355564a0.
[9] D.M. Tasset, M.F. Kubik, W. Steiner, Oligonucleotide inhibitors of human thrombin that bind distinct epitopes, J. Mol. Biol. 272 (1997) 688–698, https://doi.org/10.1006/jmbi.1997.1275.
[10] R. White, C. Rusconi, E. Scardino, A. Wolberg, J. Lawson, M. Hoffman, B. Sullenger, Generation of species cross-reactive aptamers using "toggle" SELEX, Mol. Ther. J. Am. Soc. Gene Ther. 4 (2001) 567–573, https://doi.org/10.1006/mthe.2001.0495.
[11] G. Mayer, F. Rohrbach, B. Pötzsch, J. Müller, Aptamer-based modulation of blood coagulation, Hamostaseologie 31 (2011) 258–263, https://doi.org/10.5482/ha-1156.
[12] E. Zavyalova, A. Golovin, R. Reshetnikov, N. Mudrik, D. Panteleyev, G. Pavlova, A. Kopylov, Novel modular DNA aptamer for human thrombin with high anticoagulant activity, Curr. Med. Chem. 18 (2011) 3343–3350, https://doi.org/10.2174/092986711796504727.
[13] A.V. Mazurov, E.V. Titaeva, S.G. Khaspekova, A.N. Storojilova, V.A. Spiridonova, A.M. Kopylov, A.B. Dobrovolsky, Characteristics of a new DNA aptamer, direct inhibitor of thrombin, Bull. Exp. Biol. Med. 150 (2011) 422–425, https://doi.org/10.1007/s10517-011-1158-6.
[14] E. Zavyalova, N. Samoylenkova, A. Revishchin, A. Turashev, I. Gordeychuk, A. Golovin, A. Kopylov, G. Pavlova, The evaluation of pharmacodynamics and pharmacokinetics of anti-thrombin DNA aptamer RA-36, Front. Pharmacol. 8 (2017)https://doi.org/10.3389/fphar.2017.00922.
[15] D. Kong, W. Yeung, R. Hili, In vitro selection of diversely functionalized aptamers, J. Am. Chem. Soc. 139 (2017) 13977–13980, https://doi.org/10.1021/jacs.7b07241.
[16] K. Wakui, T. Yoshitomi, A. Yamaguchi, M. Tsuchida, S. Saito, M. Shibukawa, H. Furusho, K. Yoshimoto, Rapidly neutralizable and highly anticoagulant thrombin-binding DNA aptamer discovered by MACE SELEX, Mol. Ther. Nucleic Acids. 16 (2019) 348–359, https://doi.org/10.1016/j.omtn.2019.03.002.
[17] Y. Zhou, X. Qi, Y. Liu, F. Zhang, H. Yan, DNA-nanoscaffold-assisted selection of femtomolar bivalent human α-thrombin aptamers with potent anticoagulant activity, Chembiochem Eur. J. Chem. Biol. 20 (2019) 2494–2503, https://doi.org/10.1002/cbic.201900265.
[18] P.E. Bock, P. Panizzi, I.M.A. Verhamme, Exosites in the substrate specificity of blood coagulation reactions, J. Thromb. Haemost. JTH. 5 (2007) 81–94, https://doi.org/10.1111/j.1538-7836.2007.02496.x.
[19] E. Di Cera, Thrombin, Mol. Asp. Med. 29 (2008) 203–254, https://doi.org/10.1016/j.mam.2008.01.001.
[20] N.M.-Y. Ng, N.S. Quinsey, A.Y. Matthews, D. Kaiserman, L.C. Wijeyewickrema, P.I. Bird, P.E. Thompson, R.N. Pike, The effects of exosite occupancy on the substrate specificity of thrombin, Arch. Biochem. Biophys. 489 (2009) 48–54, https://doi.org/10.1016/j.abb.2009.07.012.
[21] I. Russo Krauss, V. Napolitano, L. Petraccone, R. Troisi, V. Spiridonova, C.A. Mattia, F. Sica, Duplex/quadruplex oligonucleotides: role of the duplex domain in the stabilization of a new generation of highly effective anti-thrombin aptamers, Int. J. Biol. Macromol. 107 (2018) 1697–1705, https://doi.org/10.1016/j.ijbiomac.2017.10.033.
[22] R. Troisi, V. Napolitano, V. Spiridonova, I. Russo Krauss, F. Sica, Several structural motifs cooperate in determining the highly effective anti-thrombin activity of NU172 aptamer, Nucleic Acids Res. 46 (2018) 12177–12185, https://doi.org/10.1093/nar/gky990.
[23] I. Russo Krauss, A. Merlino, A. Randazzo, E. Novellino, L. Mazzarella, F. Sica, High-resolution structures of two complexes between thrombin and thrombin-binding aptamer shed light on the role of cations in the aptamer inhibitory activity, Nucleic Acids Res. 40 (2012) 8119–8128, https://doi.org/10.1093/nar/gks512.
[24] J. Müller, D. Freitag, G. Mayer, B. Pötzsch, Anticoagulant characteristics of HD1-22, a bivalent aptamer that specifically inhibits thrombin and prothrombinase, J. Thromb. Haemost. JTH. 6 (2008) 2105–2112, https://doi.org/10.1111/j.1538-7836.2008.03162.x.
[25] D. Kong, M. Movahedi, Y. Mahdavi-Amiri, W. Yeung, T. Tiburcio, D. Chen, R. Hili, Evolutionary outcomes of diversely functionalized aptamers isolated from in vitro evolution, ACS Synth. Biol. 9 (2020) 43–52, https://doi.org/10.1021/acssynbio.9b00222.
[26] A. Avino, C. Fabrega, M. Tintore, R. Eritja, Thrombin binding aptamer, more than a simple aptamer: chemically modified derivatives and biomedical applications, Curr. Pharm. Des. 18 (2012) 2036–2047, https://doi.org/10.2174/138161212799958387.
[27] A.M. Varizhuk, V.B. Tsvetkov, O.N. Tatarinova, D.N. Kaluzhny, V.L. Florentiev, E.N. Timofeev, A.K. Shchyolkina, O.F. Borisova, I.P. Smirnov, S.L. Grokhovsky, A.V. Aseychev, G.E. Pozmogova, Synthesis, characterization and in vitro activity of thrombin-binding DNA aptamers with triazole internucleotide linkages, Eur. J. Med. Chem. 67 (2013) 90–97, https://doi.org/10.1016/j.ejmech.2013.06.034.
[28] A. Virgilio, L. Petraccone, M. Scuotto, V. Vellecco, M. Bucci, L. Mayol, M. Varra, V. Esposito, A. Galeone, 5-Hydroxymethyl-2′-deoxyuridine residues in the thrombin binding aptamer: investigating anticoagulant activity by making a tiny chemical modification, Chembiochem Eur. J. Chem. Biol. 15 (2014) 2427–2434, https://doi.org/10.1002/cbic.201402355.
[29] W. Kotkowiak, J. Lisowiec-Wachnicka, J. Grynda, R. Kierzek, J. Wengel, A. Pasternak, Thermodynamic, anticoagulant, and antiproliferative properties of thrombin binding aptamer containing novel UNA derivative, Mol. Ther. Nucleic Acids. 10 (2018) 304–316, https://doi.org/10.1016/j.omtn.2017.12.013.
[30] G. Ying, X. Lu, J. Mei, Y. Zhang, J. Chen, X. Wang, Z. Ou, Y. Yi, A structure-activity relationship of a thrombin-binding aptamer containing LNA in novel sites, Bioorg. Med. Chem. 27 (2019) 3201–3207, https://doi.org/10.1016/j.bmc.2019.05.010.

[31] M. De Fenza, E. Eremeeva, R. Troisi, H. Yang, A. Esposito, F. Sica, P. Herdewijn, D. D'Alonzo, A. Guaragna, Structure-activity relationship study of a potent α-thrombin binding aptamer incorporating hexitol nucleotides, Chem. Weinh. Bergstr. Ger. 26 (2020) 9589–9597, https://doi.org/10.1002/chem.202001504.

[32] C. Riccardi, A. Meyer, J.-J. Vasseur, D. Cavasso, I. Russo Krauss, L. Paduano, F. Morvan, D. Montesarchio, Design, synthesis and characterization of cyclic NU172 analogues: a biophysical and biological insight, Int. J. Mol. Sci. 21 (2020)https://doi.org/10.3390/ijms21113860.

[33] I. Smirnov, N. Kolganova, R. Troisi, F. Sica, E. Timofeev, Expanding the recognition interface of the thrombin-binding aptamer HD1 through modification of residues T3 and T12, Mol. Ther. Nucleic Acids. 23 (2021) 863–871, https://doi.org/10.1016/j.omtn.2021.01.004.

[34] H.-L. Bao, T. Ishizuka, A. Yamashita, E. Furukoji, Y. Asada, Y. Xu, Improving thermodynamic stability and anticoagulant activity of a thrombin binding aptamer by incorporation of 8-trifluoromethyl-2′-deoxyguanosine, J. Med. Chem. 64 (2021) 711–718, https://doi.org/10.1021/acs.jmedchem.0c01711.

[35] J.H. Yum, T. Ishizuka, K. Fukumoto, D. Hori, H.-L. Bao, Y. Xu, H. Sugiyama, S. Park, Systematic approach to DNA aptamer design using amino acid-nucleic acid hybrids (ANHs) targeting thrombin, ACS Biomater. Sci. Eng. (2021)https://doi.org/10.1021/acsbiomaterials.1c00060.

[36] I. Russo Krauss, A. Pica, A. Merlino, L. Mazzarella, F. Sica, Duplex-quadruplex motifs in a peculiar structural organization cooperatively contribute to thrombin binding of a DNA aptamer, Acta Crystallogr. D Biol. Crystallogr. 69 (2013) 2403–2411, https://doi.org/10.1107/S0907444913022269.

[37] S.B. Long, M.B. Long, R.R. White, B.A. Sullenger, Crystal structure of an RNA aptamer bound to thrombin, RNA N. Y. N. 14 (2008) 2504–2512, https://doi.org/10.1261/rna.1239308.

[38] I. Russo Krauss, A. Merlino, C. Giancola, A. Randazzo, L. Mazzarella, F. Sica, Thrombin-aptamer recognition: a revealed ambiguity, Nucleic Acids Res. 39 (2011) 7858–7867, https://doi.org/10.1093/nar/gkr522.

[39] A. Pica, I. Russo Krauss, A. Merlino, S. Nagatoishi, N. Sugimoto, F. Sica, Dissecting the contribution of thrombin exosite I in the recognition of thrombin binding aptamer, FEBS J. 280 (2013) 6581–6588, https://doi.org/10.1111/febs.12561.

[40] I. Russo Krauss, V. Spiridonova, A. Pica, V. Napolitano, F. Sica, Different duplex/quadruplex junctions determine the properties of anti-thrombin aptamers with mixed folding, Nucleic Acids Res. 44 (2016) 983–991, https://doi.org/10.1093/nar/gkv1384.

[41] N.D. Abeydeera, M. Egli, N. Cox, K. Mercier, J.N. Conde, P.S. Pallan, D.M. Mizurini, M. Sierant, F.-E. Hibti, T. Hassell, T. Wang, F.-W. Liu, H.-M. Liu, C. Martinez, A.K. Sood, T.P. Lybrand, C. Frydman, R.Q. Monteiro, R.H. Gomer, B. Nawrot, X. Yang, Evoking picomolar binding in RNA by a single phosphorodithioate linkage, Nucleic Acids Res. 44 (2016) 8052–8064, https://doi.org/10.1093/nar/gkw725.

[42] A. Pica, I. Russo Krauss, V. Parente, H. Tateishi-Karimata, S. Nagatoishi, K. Tsumoto, N. Sugimoto, F. Sica, Through-bond effects in the ternary complexes of thrombin sandwiched by two DNA aptamers, Nucleic Acids Res. 45 (2017) 461–469, https://doi.org/10.1093/nar/gkw1113.

[43] R. Dolot, C.H. Lam, M. Sierant, Q. Zhao, F.-W. Liu, B. Nawrot, M. Egli, X. Yang, Crystal structures of thrombin in complex with chemically modified thrombin DNA aptamers reveal the origins of enhanced affinity, Nucleic Acids Res. 46 (2018) 4819–4830, https://doi.org/10.1093/nar/gky268.

[44] S.R. Stone, J. Hofsteenge, Effect of heparin on the interaction between thrombin and hirudin, Eur. J. Biochem. 169 (1987) 373–376, https://doi.org/10.1111/j.1432-1033.1987.tb13622.x.

[45] J.C. Fredenburgh, A.R. Stafford, J.I. Weitz, Evidence for allosteric linkage between exosites 1 and 2 of thrombin, J. Biol. Chem. 272 (1997) 25493–25499, https://doi.org/10.1074/jbc.272.41.25493.

[46] J.R. Koeppe, A. Seitova, T. Mather, E.A. Komives, Thrombomodulin tightens the thrombin active site loops to promote protein C activation, Biochemistry 44 (2005) 14784–14791, https://doi.org/10.1021/bi0510577.

[47] T.M. Sabo, D.H. Farrell, M.C. Maurer, Conformational analysis of gamma′ peptide (410-427) interactions with thrombin anion binding exosite II, Biochemistry 45 (2006) 7434–7445, https://doi.org/10.1021/bi060360k.

[48] T.M. Sabo, M.C. Maurer, Biophysical investigation of GpIbalpha binding to thrombin anion binding exosite II, Biochemistry 48 (2009) 7110–7122, https://doi.org/10.1021/bi900745b.

[49] N.S. Petrera, A.R. Stafford, B.A. Leslie, C.A. Kretz, J.C. Fredenburgh, J.I. Weitz, Long range communication between exosites 1 and 2 modulates thrombin function, J. Biol. Chem. 284 (2009) 25620–25629, https://doi.org/10.1074/jbc.M109.000042.

[50] I.R. Olmsted, Y. Xiao, M. Cho, A.T. Csordas, J.H. Sheehan, J. Meiler, H.T. Soh, D.J. Bornhop, Measurement of aptamer-protein interactions with back-scattering interferometry, Anal. Chem. 83 (2011) 8867–8870, https://doi.org/10.1021/ac202823m.

[51] M.V. Malovichko, T.M. Sabo, M.C. Maurer, Ligand binding to anion-binding exosites regulates conformational properties of thrombin, J. Biol. Chem. 288 (2013) 8667–8678, https://doi.org/10.1074/jbc.M112.410829.

[52] K. Chen, A.R. Stafford, C. Wu, C.H. Yeh, P.Y. Kim, J.C. Fredenburgh, J.I. Weitz, Exosite 2-directed ligands attenuate protein C activation by the thrombin-thrombomodulin complex, Biochemistry 56 (2017) 3119–3128, https://doi.org/10.1021/acs.biochem.7b00250.

[53] J. Xiao, F.R. Salsbury, Molecular dynamics simulations of aptamer-binding reveal generalized allostery in thrombin, J. Biomol. Struct. Dyn. 35 (2017) 3354–3369, https://doi.org/10.1080/07391102.2016.1254682.

[54] R. Billur, T.M. Sabo, M.C. Maurer, Thrombin exosite maturation and ligand binding at ABE II help stabilize PAR-binding competent conformation at ABE I, Biochemistry 58 (2019) 1048–1060, https://doi.org/10.1021/acs.biochem.8b00943.

[55] X. Feng, C. Yu, F. Feng, P. Lu, Y. Chai, Q. Li, D. Zhang, X. Wang, L. Yao, Direct measurement of through-bond effects in molecular multivalent interactions, Chem. Weinh. Bergstr. Ger. 25 (2019) 2978–2982, https://doi.org/10.1002/chem.201805218.

[56] R. Troisi, N. Balasco, L. Vitagliano, F. Sica, Molecular dynamics simulations of human α-thrombin in different structural contexts: evidence for an aptamer-guided cooperation between the two exosites, J. Biomol. Struct. Dyn. 39 (2021) 2199–2209, https://doi.org/10.1080/07391102.2020.1746693.

[57] Z. Otwinowski, W. Minor, Processing of X-ray diffraction data collected in oscillation mode, Methods Enzymol. 276 (1997) 307–326.

[58] A.J. McCoy, R.W. Grosse-Kunstleve, P.D. Adams, M.D. Winn, L.C. Storoni, R.J. Read, Phaser crystallographic software, J. Appl. Crystallogr. 40 (2007) 658–674, https://doi.org/10.1107/S0021889807021206.

[59] M.D. Winn, C.C. Ballard, K.D. Cowtan, E.J. Dodson, P. Emsley, P.R. Evans, R.M. Keegan, E.B. Krissinel, A.G.W. Leslie, A. McCoy, S.J. McNicholas, G.N. Murshudov, N.S. Pannu, E.A. Potterton, H.R. Powell, R.J. Read, A. Vagin, K.S. Wilson, Overview of the CCP4 suite and current developments, Acta Crystallogr. D Biol. Crystallogr. 67 (2011) 235–242, https://doi.org/10.1107/S0907444910045749.

[60] W. Bode, D. Turk, A. Karshikov, The refined 1.9-A X-ray crystal structure of D-Phe-Pro-Arg chloromethylketone-inhibited human alpha-thrombin: structure analysis, overall structure, electrostatic properties, detailed active-site geometry, and structure-function relationships, Protein Sci. Publ. Protein Soc. 1 (1992) 426–471, https://doi.org/10.1002/pro.5560010402.

[61] G.N. Murshudov, P. Skubák, A.A. Lebedev, N.S. Pannu, R.A. Steiner, R.A. Nicholls, M.D. Winn, F. Long, A.A. Vagin, REFMAC5 for the refinement of macromolecular crystal structures, Acta Crystallogr. D Biol. Crystallogr. 67 (2011) 355–367, https://doi.org/10.1107/S0907444911001314.

[62] P. Emsley, B. Lohkamp, W.G. Scott, K. Cowtan, Features and development of Coot, Acta Crystallogr. D Biol. Crystallogr. 66 (2010) 486–501, https://doi.org/10.1107/S0907444910007493.

[63] R. Improta, L. Vitagliano, L. Esposito, Peptide bond distortions from planarity: new insights from quantum mechanical calculations and peptide/protein crystal structures, PLoS One 6 (2011), e24533, https://doi.org/10.1371/journal.pone.0024533.

[64] N. Balasco, L. Esposito, L. Vitagliano, Factors affecting the amplitude of the τ angle in proteins: a revisitation, Acta Crystallogr. Sect. Struct. Biol. 73 (2017) 618–625, https://doi.org/10.1107/S2059798317007793.

[65] N. Balasco, L. Esposito, A.S. Thind, M.R. Guarracino, L. Vitagliano, Dissection of factors affecting the variability of the peptide bond geometry and planarity, Biomed. Res. Int. (2017) (2017), 2617629, https://doi.org/10.1155/2017/2617629.

[66] E. Krissinel, K. Henrick, Secondary-structure matching (SSM), a new tool for fast protein structure alignment in three dimensions, Acta Crystallogr. D Biol. Crystallogr. 60 (2004) 2256–2268, https://doi.org/10.1107/S0907444904026460.

[67] E. Krissinel, K. Henrick, Inference of macromolecular assemblies from crystalline state, J. Mol. Biol. 372 (2007) 774–797, https://doi.org/10.1016/j.jmb.2007.05.022.

[68] R.A. Laskowski, M.B. Swindells, LigPlot+: multiple ligand-protein interaction diagrams for drug discovery, J. Chem. Inf. Model. 51 (2011) 2778–2786, https://doi.org/10.1021/ci200227u.

[69] D. Van Der Spoel, E. Lindahl, B. Hess, G. Groenhof, A.E. Mark, H.J.C. Berendsen, GROMACS: fast, flexible, and free, J. Comput. Chem. 26 (2005) 1701–1718, https://doi.org/10.1002/jcc.20291.

[70] M. Parrinello, A. Rahman, Polymorphic transitions in single crystals: a new molecular dynamics method, J. Appl. Phys. 52 (1981) 7182–7190, https://doi.org/10.1063/1.328693.

[71] G. Bussi, D. Donadio, M. Parrinello, Canonical sampling through velocity rescaling, J. Chem. Phys. 126 (2007), 014101, https://doi.org/10.1063/1.2408420.

[72] T. Darden, D. York, L. Pedersen, Particle mesh Ewald: an N·log(N) method for Ewald sums in large systems, J. Chem. Phys. 98 (1993) 10089–10092, https://doi.org/10.1063/1.464397.

[73] B. Hess, H. Bekker, H.J.C. Berendsen, J.G.E.M. Fraaije, LINCS: a linear constraint solver for molecular simulations, J. Comput. Chem. 18 (1997) 1463–1472 (doi:10.1002/(SICI)1096-987X(199709)18:12%3C1463::AID-JCC4%3E3.0.CO;2-H).

[74] A. Amadei, M.A. Ceruso, A. Di Nola, On the convergence of the conformational coordinates basis set obtained by the essential dynamics analysis of proteins' molecular dynamics simulations, Proteins 36 (1999) 419–424 (doi:10.1002/(SICI)1097-0134(19990901)36:4<419::AID-PROT5>3.0.CO;2-U).

[75] W. Humphrey, A. Dalke, K. Schulten, VMD: visual molecular dynamics, J. Mol. Graph. 14 (33–38) (1996) 27–28, https://doi.org/10.1016/0263-7855(96)00018-5.

[76] R. De Cristofaro, E. Di Cera, Phenomenological analysis of the clotting curve, J. Protein Chem. 10 (1991) 455–468, https://doi.org/10.1007/BF01025473.

[77] J.R. Koeppe, E.A. Komives, Amide H/2H exchange reveals a mechanism of thrombin activation, Biochemistry 45 (2006) 7724–7732, https://doi.org/10.1021/bi060405h.

[78] L.D. Handley, B. Fuglestad, K. Stearns, M. Tonelli, R.B. Fenwick, P.R.L. Markwick, E.A. Komives, NMR reveals a dynamic allosteric pathway in thrombin, Sci. Rep. 7 (2017) https://doi.org/10.1038/srep39575.

[79] W. Yoshida, E. Mochizuki, M. Takase, H. Hasegawa, Y. Morita, H. Yamazaki, K. Sode, K. Ikebukuro, Selection of DNA aptamers against insulin and construction of an aptameric enzyme subunit for insulin sensing, Biosens. Bioelectron. 24 (2009) 1116–1120, https://doi.org/10.1016/j.bios.2008.06.016.

[80] H. Tandon, A.G. de Brevern, N. Srinivasan, Transient association between proteins elicits alteration of dynamics at sites far away from interfaces, Struct. Lond. Engl. 1993 (2020)https://doi.org/10.1016/j.str.2020.11.015.

[81] A. Cooper, D.T. Dryden, Allostery without conformational change. A plausible model, Eur. Biophys. J. EBJ 11 (1984) 103–109, https://doi.org/10.1007/BF00276625.

[82] S.M. Nimjee, S. Oney, Z. Volovyk, K.M. Bompiani, S.B. Long, M. Hoffman, B.A. Sullenger, Synergistic effect of aptamers that inhibit exosites 1 and 2 on thrombin, RNA N. Y. N. 15 (2009) 2105–2111, https://doi.org/10.1261/rna.1240109.

[83] G. La Penna, R. Chelli, Structural insights into the osteopontin-aptamer complex by molecular dynamics simulations, Front. Chem. 6 (2018) 2, https://doi.org/10.3389/fchem.2018.00002.
[84] I. Autiero, M. Ruvo, R. Improta, L. Vitagliano, The intrinsic flexibility of the aptamer targeting the ribosomal protein S8 is a key factor for the molecular recognition, Biochim. Biophys. Acta Gen. Subj. 1862 (2018) 1006–1016, https://doi.org/10.1016/j.bbagen.2018.01.014.
[85] A.A. Buglak, A.V. Samokhvalov, A.V. Zherdev, B.B. Dzantiev, Methods and applications of in silico aptamer design and modeling, Int. J. Mol. Sci. 21 (2020)https://doi.org/10.3390/ijms21228420.
[86] J. Müller, B. Wulffen, B. Pötzsch, G. Mayer, Multidomain targeting generates a high-affinity thrombin-inhibiting bivalent aptamer, Chembiochem Eur. J. Chem. Biol. 8 (2007) 2223–2226, https://doi.org/10.1002/cbic.200700535.
[87] A. Rangnekar, J.A. Nash, B. Goodfred, Y.G. Yingling, T.H. LaBean, Design of potent and controllable anticoagulants using DNA aptamers and nanostructures, Mol. Basel Switz. 21 (2016)https://doi.org/10.3390/molecules21020202.
[88] H. Hasegawa, N. Savory, K. Abe, K. Ikebukuro, Methods for improving aptamer binding affinity, Mol. Basel Switz. 21 (2016) 421, https://doi.org/10.3390/molecules21040421.
[89] Q.W. Hughes, B.T. Le, G. Gilmore, R.I. Baker, R.N. Veedu, Construction of a bivalent thrombin binding aptamer and its antidote with improved properties, Mol. Basel Switz. 22 (2017)https://doi.org/10.3390/molecules22101770.
[90] C. Riccardi, E. Napolitano, D. Musumeci, D. Montesarchio, Dimeric and multimeric DNA aptamers for highly effective protein recognition, Mol. Basel Switz. 25 (2020) https://doi.org/10.3390/molecules25225227.